Conductivity and permitivity of two-dimensional metallic photonic crystals

Andrei Pimenov, Alois Loidl

Conductivity and Permittivity of Two-Dimensional Metallic Photonic Crystals

A. Pimenov and A. Loidl

Experimentalphysik V, Center for Electronic Correlations and Magnetism, Universität Augsburg, 86135 Augsburg, Germany
(Received 3 August 2005; published 15 February 2006)

Two-dimensional metallic photonic crystals with different filling factors were manufactured and investigated by broadband terahertz spectroscopy. This technique allowed an independent determination of conductivity and dielectric permittivity in an extremely large dynamic range. Nearly ideal plasmonic behavior is observed for all compositions. Transmittance maxima are observed close to the plasma frequency and attributed to the longitudinal resonance. The plasmon frequencies agree well with existing calculations, while damping effects are underestimated by almost 1 order of magnitude.

Investigations of electrodynamic properties of photonic crystals [1,2] are motivated by the possibility to control their optical properties by changing the structural design, which is especially interesting for possible application in future optical telecommunication systems. In addition to effects like photonic band gaps and wave guiding [1,2], the possibility to obtain subwavelength resolution [3,4] using slabs of photonic crystals has been demonstrated [5,6]. These effects can be explained within the concept of negative refraction [3,7–9], formulated in the original work of Veselago [10] forty years ago.

Two-dimensional metallic photonic crystals represent a specific class of artificial crystals because in these structures the photonic gap evolve from zero frequency. This promises various possible applications especially at frequencies between microwaves and the far-infrared, like antennas, switches, or resonators. The interest in metallic photonic crystals increased substantially after the suggestion of Pendry *et al.* [11] that in these structures the classical plasmonic response of metals can be shifted into the microwave regime. The existence of a clear plasmonlike response of metallic photonic crystals has been confirmed in a number of theoretical [12–22] and experimental [23–27] studies, although the physical interpretation of this effect has been discussed controversially [21,28].

From the experimental point of view, the most readily accessible property of metallic photonic crystals is the transmittance which is strongly suppressed below the plasma frequency. In order to extract the dielectric permittivity from the experimental data, at least one additional experimental quantity is necessary. This quantity can either be the reflectance or phase shift and must be measured with high accuracy. Because of these experimental difficulties, reports on the effective dielectric permittivity of metallic photonic crystals are scarce [23,25]. In addition to the plasma frequency, another important characteristic of metallic photonic crystals is the plasmon damping. This property determines the losses in the photonic crystal and, therefore, influences such characteristics like transmitted power [29] or the quality factor of resonators.

In this Letter we systematically investigate two-dimensional metallic photonic crystals utilizing THz spectroscopy [30]. The most important and unique advantage of this technique is its tremendous dynamic range with the possibility to tune electromagnetic waves within more than a decade in frequency. The simultaneous measurement of transmission and phase shift provides direct access to conductivity and dielectric constant with high precision without relying on a Kramers-Kronig relation which always suffers from an unknown extrapolation to low and high frequencies. In addition, THz spectroscopy has a number of further advantages for spectroscopy of metallic photonic crystals. Compared to the microwave range the smaller wavelength of the radiation leads to an effective suppression of unwanted effects like crosstalk and standing waves.

Various two-dimensional metallic photonic crystals have been used in the dynamic experiments. In all cases, the length of the metallic rods was 15 mm with the cross section of samples 15×15 mm^2. Two photonic crystals were manufactured from thin Cu wires ($\o = 0.05$ mm, $\sigma_{dc} = 4.9 \times 10^5 \ \Omega^{-1} \, cm^{-1}$) using lattice spacings of 0.45 mm and 0.55 mm. The samples consisted of three rows of rods with 27 and 33 rods in the plane, respectively. To avoid the curvature of the rods, the tension of about 4 g/wire has been applied during the preparation. Other crystals with steel rods ($\sigma_{dc} = 1.7 \times 10^4 \ \Omega^{-1} \, cm^{-1}$) with $\o = 0.45$ mm, lattice spacing $a = 0.9$ mm, and with 16 rows/plane were prepared. Different thicknesses of the latter crystals (from 1 to 4 rows thick) were used to test the applicability of the effective-medium approximation. The experiments have been performed in *E* polarization (electric field parallel to the rods) and for the ΓX direction along the cube axis. Representative results in ΓM direction along the lattice diagonal will be shown for comparison.

The dynamic experiments for frequencies 60 GHz $< \nu < 380$ GHz were carried out in a Mach-Zehnder interferometer arrangement [31]. In this experimental setup transmittance ratios of more than 4 orders of magnitude
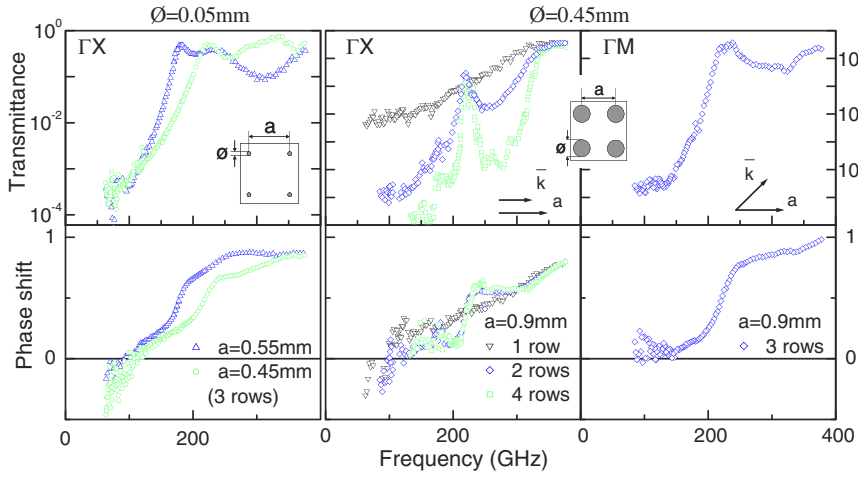
FIG. 1 (color online). Transmittance (upper panels) and phase shift (lower panels) of two-dimensional metallic photonic crystals. The phase shift is scaled to the dimensionless quantity $\varphi \rightarrow \varphi c / 2\pi d\nu$. Left panels: crystals with low filling ratio $r/a = 0.05$ mm$/0.55$ mm ($\triangle$) and $r/a = 0.05$ mm$/0.45$ mm ($\bigcirc$). Middle and right panels: crystals with high filling ratio $r/a = 0.45$ mm$/0.9$ mm and for different thicknesses and orientations as indicated.

can be measured, which, in addition to an independent determination of the phase of the radiation, is of utmost importance for the investigation of the metallic photonic crystals. Using Fresnel optical formulas for the complex transmittance [32] the absolute values of the complex conductivity $\sigma^* = \sigma_1 + i\sigma_2$ and dielectric permittivity $\varepsilon^* = \varepsilon_1 + i\varepsilon_2 = \sigma^*/i\varepsilon_0\omega$ have been determined directly from the measured spectra. Here ε_0 and $\omega = 2\pi\nu$ are the permittivity of vacuum and the angular frequency, respectively. It has been assumed that the magnetic permeability $\mu = 1$ in the frequency range of our experiments. In principle, nonmagnetic photonic crystals can have some effective magnetic permeability, e.g., due to skin effect [11,19,33], which can lead to additional effects of magnetic origin. We believe that these effects can be neglected within the present approximation, which is further supported by the thickness independence of the effective permittivity and conductivity.

Figure 1 shows transmittance and phase shift for the samples investigated. Left panels represent the data for samples with high ratio a/r (low filling ratio) and the data for high filling ratio and $a/r = 4$ are given in the middle (ΓX orientation) and right panels (ΓM orientation). In all cases the transmittance is given in absolute units and the phase shift φ is scaled by the sample thickness d and frequency ν as $\varphi \rightarrow \varphi c/2\pi d\nu$. Here c is the velocity of light. This presentation allows us to compare the phase shift of different samples on the same scale and in first approximation corresponds to the effective refractive index of the sample $n_{\text{eff}} \simeq \varphi c/2\pi d\nu$. The latter relation follows from Fresnel equations in the limit that neglects the reflections at the sample-air interface.

The transmittance of the crystals with low filling ratio (upper left panel of Fig. 1) reveals the classical features of a metal with extremely low plasma frequency: the samples are transparent above the plasma frequency and rapidly become opaque for lower frequencies. The phase shift of all samples is below unity in the complete frequency range (lower panels of Fig. 1). This indicates that the phase

velocity of light in the metallic photonic crystals is higher than the vacuum velocity.

The transmittance of photonic crystals with high filling ratio (upper middle panel of Fig. 1) is strongly suppressed already for frequencies below 320 GHz. However, the plasma frequency for these crystals is much lower, $\nu_p \simeq 230$ GHz. This difference most probably results from an overlap of the plasma resonance and the first photonic band gap (220–330 GHz) in these compositions.

Closer inspection of the transmittance data in Fig. 1 shows that all photonic crystals reveal a maximum in the vicinity of 200 GHz. As will be seen below (Table I), the frequencies of these resonances roughly correspond to the plasma frequency of the crystals. Solely the crystal with the single row of rods does not show this structure. This is not surprising taking into account that this arrangement is just a metallic grid and does not represent a "crystal." We recall that the maximum in transmittance is a typical feature of longitudinal plasma resonances and has been observed, e.g., in transmittance spectra of superconductors [34]. The effective conductivity of photonic crystals (Fig. 2) reveals a clear minimum close to the frequency of the plasma resonance which corresponds to the maximum in transmittance. Such maximum is not observed in conventional metals because the longitudinal plasmon $[\varepsilon_1(\nu_p) = 0]$ cannot couple to the (transverse) electromagnetic radiation. This difference remains unresolved at this stage and might arise due to shortcomings of the effective-medium approximation for metallic photonic crystals.

The effective conductivity and dielectric constant of the photonic crystals as calculated from transmittance and phase shift are represented in Fig. 2. All notations are the same as in Fig. 1. Dashed lines in Fig. 2 represent calculations of the dielectric function of a plasmon in a Drude-metal:

$$\varepsilon^* = \varepsilon_1 + i\frac{\sigma_1}{\varepsilon_0\omega} = \varepsilon_\infty - \frac{\omega_p^2}{\omega(\omega + i/\tau)}, \qquad (1)$$

where $\omega_p = 2\pi\nu_p$ is the plasma frequency, τ is the scat-

TABLE I.   Parameters of the plasma resonances in two-dimensional metallic photonic crystals
[Eq. (1)]. $\sigma(0) = \varepsilon_0 \omega_p^2 \tau$ is the effective dc conductivity of the plasmon. The experimentally
determined plasma frequency is compared to the calculations using Eq. (2).

$\frac{a(mm)}{\text{ø}(mm)}$	ν_p (GHz)		$1/2\pi\tau$ (GHz)	$\sigma(0)$ (Ω^{-1} cm^{-1})
	Experiment	Equation (2)		
$\frac{0.55}{0.05}$	155	153	11	1.2
$\frac{0.45}{0.05}$	192	197	21	1.0
$\frac{0.9}{0.45}$, ΓX	225	233	14	2.0
$\frac{0.9}{0.45}$, ΓM	230	233	11	2.7

tering rate, and $\varepsilon_\infty \sim 1$ is the high-frequency dielectric
constant. In the case of low damping, the dielectric con-
stant close to the plasma frequency takes the form $\varepsilon_1 =
\varepsilon_\infty - \nu_p^2/\nu^2$. This approximation works well for the data
in Fig. 2: in the full frequency range the dielectric constant
reveals well-defined plasmonlike behavior.

For frequencies above 200 GHz the conductivity spectra
reveal additional maxima which are related to photonic
band gaps. These structures directly correspond to the
minima in transmittance between the allowed photonic
bands. As a first approximation, the conductivity maxima
have been taken into account in the fits by additional
Lorentzians with frequencies corresponding to the local
maxima of the conductivity and are shown as solid lines in
Fig. 2. In addition, dashed lines in Fig. 2 represent pure
plasmon behavior, Eq. (1). Both models coincide at low
frequencies and in $\varepsilon(\nu)$ the differences are hardly seen at
all. The damping of the plasmon is basically determined by
the real part of the conductivity below 200 GHz and is only
weakly influenced by the Lorentzians. The parameters of
the plasmon in Fig. 2 are given in Table I. The fits clearly
indicate that the plasmon is well defined for all samples
investigated, i.e., $\nu_p \gg 1/2\pi\tau$. We note that even the
effective dielectric constant of a metal grid, formally cal-
culated with the thickness $d = 1 \times a$, follows the data of
the photonic crystals with the same plasma frequency.

The conductivity and dielectric permittivity of photonic
crystals with different thicknesses shown in the middle
panels of Fig. 2 agree within experimental accuracy. The

difference in dielectric constants at lowest frequencies is
due to experimental uncertainties in measuring the trans-
mittance for the crystal with 4 rows. The thickness inde-
pendence of the data demonstrates that the concept of
effective medium for metallic photonic crystals works
rather well below and above the plasma frequency. An
additional support for this concept is provided by the
direction independence (ΓX versus ΓM) of the data. As
discussed above, the appearance of the conductivity mini-
mum close to the plasma frequency indicates that some
corrections to the effective-medium approximation never-
theless might be necessary.

The effective plasma frequency of photonic crystals has
been calculated within different approximations and is well
documented in literature. The comparison [20–22] of vari-
ous analytical expressions and numerical calculations
shows the basic agreement between the computational
results. For the sake of simplicity we compare our experi-
mental results with the expression of Ref. [19]

$$\nu_p^2 = \frac{c^2}{\pi a^2 [2 \ln(\sqrt{2}a/\text{ø}) + \pi/2 - 3]}. \qquad (2)$$

Equation (2) corresponds to the limit of strong skin effect,
i.e., $\delta \ll \text{ø}$. Here $\delta = \sqrt{2/\mu_0 \omega \sigma_{dc}}$ is the skin depth, μ_0
the permeability of vacuum, and σ_{dc} is the dc conductivity
of the rod material. The values of the plasma frequency
calculated from Eq. (2) are compared to the experimental
data in Table I. Equation (2) reproduces the experimentally
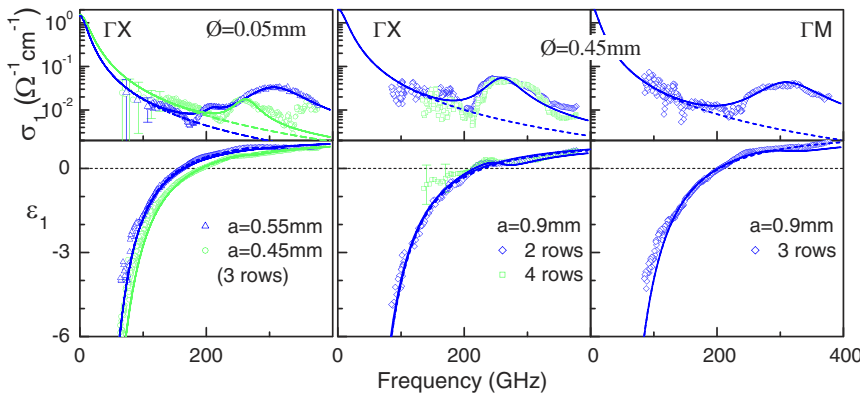observed plasma frequencies within 4% in all cases. This

FIG. 2 (color online).   Effective con-
ductivity (σ_1, upper panels) and dielec-
tric constant (ε_1, lower panels) of two-
dimensional metallic photonic crystals.
The experimental geometry and nota-
tions are the same as in Fig. 1. Left
panels—crystals with low filling ratio.
Middle and right panels—crystals with
high filling ratio. Dashed lines corre-
spond to pure plasmon behavior,
Eq. (1). Solid lines represent fits includ-
ing Lorentzians to account for the pho-
tonic band gaps.

result could be expected since the penetration depth estimated for $\nu = 200$ GHz is $\delta \sim 1.6 \times 10^{-4}$ mm for Cu wires and $\delta \sim 9 \times 10^{-4}$ mm for steel rods. Therefore, the limit of strong skin effect should work well for all three compositions.

Contrary to the good agreement between experimental and theoretical values for the plasma frequency, the experimentally determined scattering rates do not agree with the model calculations. An estimate of the scattering rate in the limit of strong skin effect can be obtained from Eq. (15) of Ref. [11] replacing the cross section of the rods $\pi \o^2/4$ (no skin effect) by the effective cross section $\pi \o \delta$ (strong skin effect). The resulting expressions then read:

$$\frac{1}{2\pi\tau} = \frac{2a^2}{\o\delta} \frac{\varepsilon_0 \nu_p^2}{\sigma_{\mathrm{dc}}} \quad \text{and} \quad \sigma(0) = \sigma_{\mathrm{dc}} \pi \o \delta/a^2. \quad (3)$$

Here σ_{dc} is the dc conductivity of the rods material. The arguments given in Ref. [19] describing the limit of strong skin effect lead to an expression which coincides with Eq. (3) up to a numerical factor of the order of unity. An estimate based on Eq. (3) leads to the scattering rates $1/2\pi\tau$ between 0.2 and 0.7 GHz. These values are more than order of magnitude too low compared to the experimental data. Similar discrepancies arise between the experimental conductivity of the plasmon (last column of Table I) and the effective conductivity calculated from Eq. (3). The estimates yield values ~ 50 $\Omega^{-1}\,\mathrm{cm}^{-1}$ for copper photonic crystals and ~ 30 $\Omega^{-1}\,\mathrm{cm}^{-1}$ for the steel samples, which again differs by more than 1 order of magnitude from the experiment. Further theoretical and experimental efforts are needed to clarify this discrepancy. Finally, we note that Eq. (3) leads to a frequency-dependent scattering rate and therefore would result in a modified frequency dependence of the conductivity in Eq. (1). In the limit $\omega\tau \gg 1$ this yields $\sigma_1 \propto \omega^{3/2}$, compared to $\sigma_1 \propto \omega^2$ in Eq. (1). Taking into account the scattering of the conductivity data in Fig. 2 we cannot distinguish between these two power laws.

In summary, electrodynamic properties of two-dimensional metallic photonic crystals have been investigated for different compositions and in the broad frequency range from 60 GHz to 380 GHz. For all compositions investigated both dielectric permittivity and dispersion relations reveal plasmonic behavior. Good agreement with existing theories is obtained concerning the position of the plasma resonances in these structures. On the contrary, the effective conductivity of the photonic crystals and the plasmon damping differ by more than 1 order of magnitude from theoretical predictions. Finally, characteristic maxima in the transmittance have been observed for all compositions and attributed to the longitudinal plasma resonance.

[1] K. Sakoda, *Optical Properties of Photonic Crystals* (Springer, New York, 2001).
[2] S. G. Johnson and J. D. Joannopoulos, *Photonic Crystals: The Road from Theory to Practice* (Kluwer Academic Publishers, Dordrecht, 2002).
[3] J. B. Pendry, Phys. Rev. Lett. **85**, 3966 (2000).
[4] See D. R. Smith, J. B. Pendry, and M. C. K. Wiltshire, Science **305**, 788 (2004) and references therein.
[5] E. Cubukcu et al., Phys. Rev. Lett. **91**, 207401 (2003).
[6] P. V. Parimi et al., Nature (London) **426**, 404 (2003).
[7] E. Cubukcu et al., Nature (London) **423**, 604 (2003).
[8] S. Foteinopoulou, E. N. Economou, and C. M. Soukoulis, Phys. Rev. Lett. **90**, 107402 (2003).
[9] R. A. Shelby, D. R. Smith, and S. Schultz, Science **292**, 77 (2001).
[10] V. G. Veselago, Sov. Phys. Usp. **10**, 509 (1968).
[11] J. B. Pendry et al., Phys. Rev. Lett. **76**, 4773 (1996).
[12] K. Sakoda et al., Phys. Rev. B **64**, 045116 (2001).
[13] D. R. Smith et al., Phys. Rev. B **65**, 195104 (2002).
[14] M. M. Sigalas et al., Phys. Rev. B **52**, 11 744 (1995).
[15] P. A. Belov, C. R. Simovski, and S. A. Tretyakov, Phys. Rev. E **66**, 036610 (2002).
[16] V. Kuzmiak, A. A. Maradudin, and F. Pincemin, Phys. Rev. B **50**, 16 835 (1994); V. Kuzmiak and A. A. Maradudin, ibid. **55**, 7427 (1997); **58**, 7230 (1998).
[17] A. A. Krokhin and E. Reyes, Phys. Rev. Lett. **93**, 023904 (2004).
[18] G. Guida et al., J. Opt. Soc. Am. B **15**, 2308 (1998).
[19] A. K. Sarychev and V. M. Shalaev, Phys. Rep. **335**, 275 (2000); cond-mat/0103145.
[20] P. Markoš and C. M. Soukoulis, Opt. Lett. **28**, 846 (2003).
[21] A. L. Pokrovsky and A. L. Efros, Phys. Rev. Lett. **89**, 093901 (2002).
[22] A. L. Pokrovsky, Phys. Rev. B **69**, 195108 (2004).
[23] A. F. Starr et al., Phys. Rev. B **70**, 113102 (2004).
[24] P. Gay-Balmaz, C. Maccio, and O. J. F. Martin, Appl. Phys. Lett. **81**, 2896 (2002).
[25] F. J. Rachford et al., Phys. Rev. E **66**, 036613 (2002).
[26] E. Ozbay et al., IEEE Trans. Antennas Propag. **51**, 2592 (2003).
[27] J. B. Pendry et al., J. Phys. Condens. Matter **10**, 4785 (1998).
[28] S. A. Mikhailov, Phys. Rev. Lett. **78**, 4135 (1997); J. B. Pendry et al., ibid. **78**, 4136 (1997); R. M. Walser, A. P. Valanju, and P. M. Valanju, ibid. **87**, 119701 (2001).
[29] E. V. Ponizovskaya, M. Nieto-Vesperinas, and N. Garcia, Appl. Phys. Lett. **81**, 4470 (2002).
[30] H. Němec et al., Appl. Opt. **43**, 1965 (2004); F. Gadot et al., J. Appl. Phys. **85**, 8499 (1999).
[31] A. A. Volkov et al., Infrared Phys. **25**, 369 (1985).
[32] O. S. Heavens, *Optical Properties of Thin Solid Films* (Dover, New York, 1991).
[33] M. L. Povinelli, S. G. Johnson, J. D. Joannopoulos, and J. B. Pendry, Appl. Phys. Lett. **82**, 1069 (2003); C.-S. Kee et al., Phys. Rev. E **59**, 4695 (1999).
[34] A. Pimenov et al., Phys. Rev. Lett. **87**, 177003 (2001); Appl. Phys. Lett. **77**, 429 (2000).